Calculation of dispersion in graded-index multimode fibers by a propagating-beam method

M. D. Feit and J. A. Fleck, Jr.

Methods are developed for extracting from a numerical propagating-beam solution of a scalar wave equation the information necessary to compute the impulse-response function and the pulse dispersion for a multimode graded-index fiber. It is shown that the scalar Helmholtz equation and the parabolic wave equation have the same set of eigenfunctions in common and that the eigenvalues for the two equations are simply related. Thus one can work exclusively with the simpler parabolic equation. Both the mode eigenvalues (propagation constants) and mode weights, which are necessary for determining the impulse response, can be obtained with high accuracy from a numerical Fourier transform of the complex field-correlation function by the use of digital-filtering techniques. It is shown how a solution obtained in the absence of profile dispersion can be simply corrected for the presence of profile dispersion. In an illustrative example a graded-index fiber with a central dip in its profile is considered.

I. Introduction

In an earlier publication,[1] we described an accurate method for computing the electric field in an optical waveguide that circumvents the usual field synthesis in terms of normal modes. The method relies on a discrete Fourier representation of the field and solves the scalar Helmholtz equation by a marching algorithm that can accurately treat realistic source conditions. The solution gives all the spatial and angular properties of a beam that originates from a prescribed source distribution and propagates down the waveguide. In addition, the Fourier transform of the field with respect to axial distance z at a single transverse point (x,y) yields the totality of all mode eigenvalues β_n, including those that correspond to leaky or decaying modes. This method of solution will hereafter be referred to as the propagating-beam method. In this paper we show how the propagating-beam method can be applied to the calculation of pulse dispersion in multimode fibers.

The behavior of a pulse transmitted along a length z of optical fiber is conveniently characterized by the impulse-response function[2]

$$h(t,z) = \sum_n W_n \, \delta(t - z/v_n), \tag{I.1}$$

where the coefficients W_n represent the relative power in the fiber modes that are excited and the v_n are the mode-group velocities defined by the relation

$$1/v_n = \partial\beta_n/\partial\omega. \tag{I.2}$$

If the intramodal contributions to pulse broadening are neglected, the time dependence of a pulse after propagating a distance z can be represented in terms of its shape at $z = 0$ through the convolution

$$f(t,z) = \int_0^t h(t',z)\, f(t - t',0)\, dt'. \tag{I.3}$$

Determination of the dispersion for a specific fiber and set of launch conditions thus reduces to the computation of the mode-group velocities v_n and the mode weights W_n.

Mode-group velocities have been calculated with a variety of techniques, including the WKB method,[2–5] perturbation theory,[4–6] evanescent-wave theory,[7] and the simultaneous numerical computation of mode eigenvalues and eigenfunctions.[8–11] The selection of the mode weights W_n, on the other hand, has traditionally been based on heuristic assumptions, for example, that all modes with the same principal mode number are excited with equal power.[12] Such an assumption may be justified if sufficient mode mixing takes place within the fiber.[13] There may be situations, however, in which it is desirable to have the mode weights determined by source and launch conditions. If the set of normalized eigenfunctions for all guided modes is available, say, from a numerical computation, it is possible, at least in principle, to expand the field at $z = 0$ in a series of these functions. If the expansion coefficients are A_n, the power in the mode designated by n is proportional to

The authors are with University of California, Lawrence Livermore Laboratory, Livermore, California 94550.

Received 8 March 1979.

$|A_n|^2$. To our knowledge, however, this procedure has never been carried out.

The propagating-beam method, as already mentioned, is capable of furnishing the mode eigenvalues β_n at the same time that it is generating a variety of other data. Computation of the field for two or more values of ω permits the numerical evaluation of the derivatives in Eq. (I.2). It is also possible to determine from a propagating-beam solution the sum of the weights of all modes belonging to a set with the same propagation constant. Knowing the total weight of each such degenerate mode set and the corresponding group velocity is sufficient for computing the impulse-response function (I.1). Two methods are available for determining the weights. The first method requires squaring the complex field amplitude and integrating over the fiber cross section for each increment in z. The resulting complex function of z is then Fourier transformed numerically, and the heights of the peaks of the resulting spectrum will be proportional to the desired weights. The second method, which is the more accurate of the two, is based on a correlation function formed by multiplying the conjugate of the complex field amplitude at $z = 0$ and the complex field amplitude for arbitrary z and integrating over the fiber cross section. The numerical Fourier transform with respect to z of the complex correlation function, applied in conjunction with digital-filtering techniques, gives highly accurate values for both the mode weights and eigenvalues, where the former are determined by the heights of the peaks and the latter by their position.

The paper is organized as follows. In Sec. II it is shown that the eigenfunctions for the parabolic approximation to the Helmholtz equation are identical to those of the Helmholtz equation itself and that the eigenvalues for the two equations are simply related. Methods for determining mode weights under general launch conditions are derived in Sec. III. The accuracy of the determination of mode weights, propagation constants, and group delays is also assessed in Sec. III. An application of the techniques developed is discussed in Sec. IV. In the example considered, a multimode fiber with a central dip in its refractive index is irradiated by an incoherent beam. Conclusions are stated in Sec. V, and in the Appendix an equation is derived relating group velocities in the presence of profile dispersion to those computed without it.

II. Relationship Between Eigenfunctions and Eigenvalues of the Helmholtz and Parabolic Equations

It is assumed that the propagation of a single-frequency component of light is governed by the scalar Helmholtz equation

$$\frac{\partial^2 E}{\partial x^2}+\frac{\partial^2 E}{\partial y^2}+\frac{\partial^2 E}{\partial z^2}+\frac{\omega^2}{c^2}n^2(\omega,x,y)E=0, \tag{1}$$

where $E(\omega,x,y,z)\exp(i\omega t)$ is the transverse component of the electric field at angular frequency ω, and $n(\omega,x,y)$ is the refractive index. It will be convenient to extract from the z dependence of $E(\omega,x,y,z)$ a carrier wave moving in the positive z direction. Thus we write

$$E(\omega,x,y,z)=\mathcal{E}(\omega,x,y,z)\exp(-ikz), \tag{2}$$

where

$$k=(n_0\omega)/c, \tag{3}$$

and n_0 is some reference value of the refractive index, which we take here to be that of the fiber cladding.

Substitution of Eq. (2) into Eq. (1) yields the following equation for the complex field amplitude $\mathcal{E}$:

$$-\frac{\partial^2\mathcal{E}}{\partial z^2}+2ik\frac{\partial\mathcal{E}}{\partial z}=\nabla_\perp^2\mathcal{E}+k^2\left[\left(\frac{n}{n_0}\right)^2-1\right]\mathcal{E}, \tag{4}$$

where $\nabla_\perp^2=\partial^2/\partial x^2+\partial^2/\partial y^2$. Neglect of the first left-hand member of Eq. (4) yields the parabolic or Fresnel form of the wave equation

$$2ik\frac{\partial\mathcal{E}'}{\partial z}=\nabla_\perp^2\mathcal{E}'+k^2\left[\left(\frac{n}{n_0}\right)^2-1\right]\mathcal{E}'. \tag{5}$$

Hereafter we shall use a prime to distinguish between solutions of the parabolic and the scalar Helmholtz equations.

It is easy to show that the Helmholtz equation [Eq. (4)] and the parabolic equation [Eq. (5)] have the same set of eigenfunctions in common and that eigenvalues for the Helmholtz equation can be simply obtained from those of the parabolic equation. To this end, we write the solution to the Helmholtz equation as

$$\mathcal{E}(x,y,z)=u_n(\mathbf{x})\exp(-i\beta_n z), \tag{6}$$

where $\mathbf{x}\equiv(x,y)$, and the solution to the Fresnel equation as

$$\mathcal{E}'(x,y,z)=u_n'(\mathbf{x})\exp(-i\beta_n' z). \tag{7}$$

Here for simplicity we have used a single index label n to distinguish the different modes. Substitution of Eqs. (6) and (7) into Eqs. (4) and (5), respectively, gives

$$(\beta_n^2+2k\beta_n)u_n=\nabla_\perp^2 u_n+k^2\left\{\left[\frac{n(x,y)}{n_0}\right]^2-1\right\}u_n, \tag{8a}$$

$$2k\beta_n' u_n'=\nabla_\perp^2 u_n'+k^2\left\{\left[\frac{n(x,y)}{n_0}\right]^2-1\right\}u_n'. \tag{8b}$$

Clearly $u_n(\mathbf{x})\equiv u_n'(\mathbf{x})$, since the operators on the right-hand sides of both Eqs. (8a) and (8b) are identical. Furthermore, β_n and β_n' are related through the expressions

$$\beta_n'=(\beta_n^2+2k\beta_n)/2k, \tag{9a}$$

$$\beta_n=-k\left[1-(1+2\beta_n'/k)^{1/2}\right]=\beta_n'-\frac{1}{2}\frac{\beta_n'^2}{k}+\ldots. \tag{9b}$$

Thus to determine the eigenvalues for the Helmholtz equation it is sufficient to determine them for the Fresnel equation and to apply Eq. (9b). [The reader is reminded that the propagation constants appearing in Eqs. (6)–(9) have had the carrier wave contribution k removed, and in this respect they differ from the propagation constants used in conventional waveguide literature.] These results can be very useful, since it is often more convenient to work with the parabolic equation than the Helmholtz equation.

From Eq. (9) we have

Table I. Comparison of Numerically and Analytically Calculated Propagation Constants and Group Delays for Square-Law Refractive Medium

n	β_n (cm^{-1}) Numerical	Analytical	$\left(\frac{1}{v_n}-\frac{\partial\beta_n'}{\partial\omega}\right)$ (psec/km) Numerical	Analytical
0	713.6	712.6	159.56	159.54
1	672.7	672.2	158.17	158.15
2	631.8	631.8	155.84	155.84
3	590.9	591.2	152.57	152.60
4	549.9	550.8	148.34	148.45
5	511.6	510.3	143.54	143.36
6	470.6	469.8	137.48	137.35
7	429.7	429.3	130.48	130.41
8	388.8	388.9	122.55	122.57
9	347.9	348.4	113.67	113.78
10	306.9	307.9	103.82	104.07
11	266.0	267.4	93.06	93.44
12	227.7	227.0	82.12	81.91
13	186.7	186.5	69.49	69.43
14	145.8	146.0	55.95	56.02
15	104.9	105.5	41.46	41.68
16	64.0	65.1	26.04	26.46
17	25.6	24.6	10.69	10.28

$$\frac{1}{v_n}=\frac{\partial\beta_n}{\partial\omega}=\frac{n_0}{c}\left\{\frac{\left(1+\frac{\beta_n'}{k}+\frac{c}{n_0}\frac{\partial\beta_n'}{\partial\omega}\right)}{\left(1+\frac{2\beta_n'}{k}\right)^{1/2}}-1\right\}. \tag{10}$$

To second order in β_n'/k Eq. (10) can be written as

$$\frac{1}{v_n}\cong\left[1-\frac{\beta_n'}{k}+\frac{3}{2}\left(\frac{\beta_n'}{k}\right)^2\right]\frac{\partial\beta_n'}{\partial\omega}+\frac{1}{2}\frac{n_0}{c}\left(\frac{\beta_n'}{k}\right)^2. \tag{11}$$

The group delays $\tau_n = v_n^{-1}$, which appear in Eq. (11), are expressed relative to the delay for the carrier wave, n_0/c.

To compute the β_n' from a numerical solution of Eq. (5), it is necessary to calculate the Fourier transform of $\mathcal{E}'(\omega,x,y,z)$ for a particular transverse position (x,y) not at the origin. If we call this Fourier transform $\mathcal{E}'(\omega,x,y,\beta)$, the spectral density $|\mathcal{E}'(\omega,x,y,\beta)|^2$ will display a set of sharp resonant peaks, which can be identified with the guided modes of the fiber. By identifying the values of β corresponding to these maxima, one can determine the β_n'. There is, of course, an implied uncertainty in the values of β_n' so determined, if they are picked from a discrete set of values of a numerical transform. The maximum uncertainty in β_n' can be expressed in terms of the sampling interval $\Delta\beta$ along the β axis and the propagation distance Z over which the solution $\mathcal{E}'(\omega,x,y,z)$ is available as

$$\Delta\beta_n'=\frac{1}{2}\Delta\beta=\pi/Z. \tag{12}$$

A resolution of 1 cm^{-1} in the determination of β_n' according to Eq. (12) requires a propagation distance of about 3 cm. It is possible, however, to improve substantially on the accuracy implied in Eq. (12) by multiplying the data sample to be Fourier transformed by a suitable window[14] function and then selecting the β_n' values from the transformed sample by interpolation.[15]

Table I shows the results of a numerical computation of the propagation constants and mode-group velocities based on a numerical solution of Eq. (5), the spectral density $|\mathcal{E}'(\omega,x,y,\beta)|^2$ for an off-axis point, and Eq. (10). The fiber was assumed to have a truncated square-law profile defined by

$$n^2=\begin{cases}n_1^2\left[1-2\Delta\left(\frac{r}{a}\right)^2\right] & r\le a\\ n_0^2=(1-2\Delta)n_1^2 & r\ge a\end{cases}, \tag{13}$$

with $\Delta = 0.008$, $a = 31.25$ μm, and $n_0 = 1.5$. The vacuum wavelength λ was taken to be 1 μm, and the total propagation distance was $Z = 2.45$ cm. The β_n' were determined by selecting the local maxima of $|\mathcal{E}'(\omega,x,y,\beta)|^2$ without benefit of interpolation. In Eq. (10) the numerically determined eigenvalues β_n' were used, but the derivatives $\partial\beta_n'/\partial\omega$ were calculated by differentiating the analytic expression

$$\beta'(m,n)=\frac{\Delta n_1^2}{n_0}\frac{\omega}{c}-\frac{n_1}{n_0}\frac{(2\Delta)^{1/2}}{a}(m+n+1). \tag{14}$$

Also displayed in Table I for comparison are the propagation constants and group delays from the Helmholtz equation for an infinite square-law medium. The latter values were computed from the analytic expression[16]

$$\beta(m,n)=-n_0\frac{\omega}{c}+n_1\frac{\omega}{c}\left[1-\frac{2c(2\Delta)^{1/2}}{n_1\omega a}(m+n+1)\right]^{1/2}. \tag{15}$$

In Table I it is seen that the numerically and analytically determined values of β_n agree to within the 1-cm^{-1} resolution predicted by Eq. (12).[17] The corresponding values for group delays are in good over-all agreement. These results give confidence that propagation constants can be determined with sufficient precision by the propagating-beam method for an accurate calculation of pulse dispersion.

For more general refractive index profiles $n(r)$ can be written as

$$n^2=\begin{cases}n_1^2\left[1-2\Delta f\left(\frac{r}{a}\right)\right] & r\le a\\ n_0^2=(1-2\Delta)n_1^2 & r\ge a\\ f(0)=0 & \\ f\left(\frac{r}{a}\right)=1, r\ge a & \end{cases}. \tag{16}$$

In general, it will be necessary to evaluate the propagation constants β_n' for at least two different values of ω in order to compute the derivatives $\partial\beta_n'/\partial\omega$ numerically. This will require solving Eq. (5) for each value of ω. In doing so, one should consider not only the explicit dependence of Eq. (5) on ω, but also the detailed variation of the profile function with ω. This method will thus allow a completely general treatment of dispersion if appropriate refractive index data are available.

A simple model of profile dispersion[2,18] is based on the assumption that the parameter Δ depends on wavelength, while the function $f(r/a)$ is independent of

it. In this case one can ignore the presence of profile dispersion in calculating the mode-group delays $\partial\beta_n'/\partial\omega$ and correct for it afterwards. If we call $\beta_n'^0$ the propagation constants calculated without profile dispersion, it can be shown (see Appendix) that the group delays in the presence of profile dispersion are given by the expression

$$\frac{\partial\beta_n'}{\partial\omega} = \frac{\partial\beta_n'^0}{\partial\omega}\left(1 - \lambda\frac{\partial \ln n_1}{\partial\lambda} - \frac{1}{2}\lambda\frac{\partial \ln\Delta}{\partial\lambda}\right) - \frac{\beta_n'^0}{\omega}\left(\frac{1}{2} + \frac{\Delta}{1-\Delta}\right)\lambda\frac{\partial \ln\Delta}{\partial\lambda}. \quad (17)$$

III. Determination of Mode Weights for Arbitrary Launch Conditions

A. Method 1 (Field-Squared Method)

The complex field amplitude $\mathcal{E}(x,y,z)$ can be expressed in terms of the waveguide-mode eigenfunctions as

$$\mathcal{E}(x,y,z) = \sum_{n,j} A_{nj}\, u_{nj}(\mathbf{x}) \exp(-i\beta_n z). \quad (18)$$

The index j is used here to distinguish different members of the degenerate mode set that may have the same propagation constant β_n. Squaring $\mathcal{E}$, integrating over the total fiber cross section, and taking account of the orthogonality of the set of eigenfunctions give

$$\mathcal{P}(z) = \int\int \mathcal{E}^2(x,y,z)dxdy = \sum_{n,j} A_{nj}^2 \exp(-2i\beta_n z). \quad (19)$$

The Fourier transform of $\mathcal{P}(z)$ is

$$\mathcal{P}(\beta) = \sum_{n,j} A_{nj}^2\, \delta(\beta - 2\beta_n). \quad (20)$$

Let us assume for the moment that the A_n are all real. If we now identify the W_n as the total weight of all modes having the same propagation constant β_n, the W_n satisfy

$$W_n = \text{const} \times \sum_j A_{nj}^2. \quad (21)$$

Thus the mode weights W_n can be determined from the heights of the maxima in the function $\mathcal{P}(\beta)$. In practice $\mathcal{P}(\beta)$ must be computed from a finite set of discrete $\mathcal{P}(z)$ values that have been multiplied by a suitable window function.[14] The peaks in $\mathcal{P}(\beta)$ will display a finite width and shape that are characteristic of both the window function and the propagation distance.

Table II shows the results of a mode-weight determination based on the field-squared method for a Gaussian beam introduced into a 1-D quadratic refracting medium. The refractive index was of the form (14) with x substituted for r. The value of a was taken to be 31.25 μm, and the quadratic dependence on x was continued to the edge of the computational grid at $x = \pm 120$ μm. The remaining parameters were as for Eq. (14). The beam shape at $z = 0$ was taken to be the Gaussian $\mathcal{E}(x,0) = \exp(-x^2/2\sigma^2)$ with $\sigma = 10.24$ μm. The appropriate mode eigenfunctions for this problem are[16]

$$u_n(x) = (\pi^{1/2}2^n n!)^{1/2} H_n(x/\sigma_a) \exp(-x^2/2\sigma_a^2), \quad (22)$$

where the $H_n(x)$ are Hermite polynomials and

$$\sigma_a = \left[\frac{a}{k(2\Delta)^{1/2}}\right]^{1/2}. \quad (23)$$

Table II shows the ratio A_n^2/A_0^2 for an expansion in terms of the eigenfunctions (22), calculated both analytically and numerically using Eqs. (5) and (21), for a propagation distance of 9.5 cm. The analytic coefficients were computed from

$$A_{2n} = \left[\frac{2n!}{\pi 2^{2n-1}(1+b^2)}\right]^{1/2}\left(\frac{1-b^2}{1+b^2}\right)^n \frac{1}{n!}, \quad (23a)$$

where $b = \sigma_a/\sigma$.

In the numerical calculation a Hanning[19] window and quadratic interpolation were used.

The procedure just outlined can be generalized to the case where the A_{nj} are complex. Let

$$A_{nj} = A_{nj}^{\mathcal{R}} + iA_{nj}^{\mathcal{I}}. \quad (24)$$

Then it will be necessary to run two separate propagation calculations with $\mathcal{E}'(x,y,0) = \mathcal{R}_e[\mathcal{E}(x,y,0)]$ and $\mathcal{I}_m[\mathcal{E}(x,y,0)]$, respectively, as starting conditions. Applying Eqs. (19)–(21) to both calculations will allow one to determine W_n as

$$W_n = \sum_j (A_{nj}^{\mathcal{R}})^2 + \sum_j (A_{nj}^{\mathcal{I}})^2 = \sum_j [(A_{nj}^{\mathcal{R}})^2 + (A_{nj}^{\mathcal{I}})^2]. \quad (25)$$

B. Method 2 (Correlation-Function Method)

Let us form the product $\mathcal{E}^*(x,y,0)\mathcal{E}(x,y,z)$ and integrate over the cross section of the fiber. Making use of Eq. (18), we have

$$\mathcal{P}_1(z) = \int\int \mathcal{E}^*(x,y,0)\mathcal{E}(x,y,z)dxdy = \langle \mathcal{E}^*(x,y,0)\mathcal{E}(x,y,z)\rangle = \sum_{n,j} |A_{nj}|^2 \exp(-i\beta_n z). \quad (26)$$

Taking the Fourier transform of Eq. (26) gives

$$\mathcal{P}_1(\beta) = \sum_{n,j} |A_{nj}|^2\, \delta(\beta - \beta_n). \quad (27)$$

The maxima of $\mathcal{P}_1(\beta)$, determined for a single propagation calculation, give the desired weights,

$$W_n = \text{const} \times \sum_j |A_{nj}|^2, \quad (28)$$

even for A_{nj} complex.

Table III shows the results of a mode-weight determination with the correlation-function method for the conditions of Table II, except that a four-term Blackman-Harris[14,20] window was employed. Best results were obtained with quadratic interpolation. The

Table II. Comparison of Analytically and Numerically Determined Mode Weights for 1-D Square-Law Refracting Medium Illuminated by Gaussian Beam, Using $\mathcal{E}^2$ Method, Hanning Window, and Quadratic Interpolation

n	A_n^2/A_0^2 Analytical	A_n^2/A_0^2 Numerical
2	0.1800	0.1765
4	0.0486	0.0443
6	0.0146	0.0118
8	0.0046	0.0031
10	0.0015	0.0008

Table III. Comparison of Analytically and Numerically Determined Mode Weights Using Correlation-Function Method [a]

n	A_n/A_0^2 Analytical	A_n/A_0^2 Numerical
2	0.1800	0.1805
4	0.0486	0.0489
6	0.0146	0.0147
8	0.0046	0.0046
10	0.0015	0.0015

[a] Same conditions as for Table II but with four-term Blackman-Harris window.

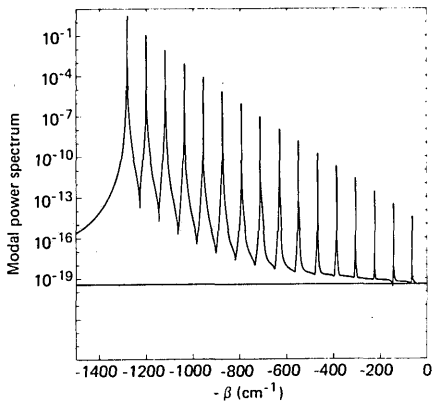

Fig. 1. Fourier transform of complex field-correlation function for Gaussian beam propagating in a 1-D quadratic refracting medium. Heights of spectral peaks are proportional to the weights of normal modes excited.

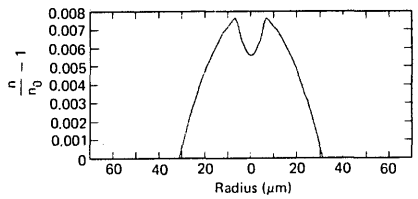

Fig. 2. Refractive index as a function of radius. Parabolically shaped dip in center of quadratically varying index profile.

over-all agreement between the numerical and analytic results is excellent. The agreement is particularly impressive considering the small amounts of power that are contained in the higher modes. The power spectrum $\mathcal{P}_1(\beta)$ calculated for a Hanning window is shown in Fig. 1, plotted vs $-\beta$ (to emphasize the similarity between an optical waveguide and a quantum-mechanical system with an attractive potential). Figure 1 gives an accurate picture of both the relative mode powers and their eigenvalues.

Table IV gives a comparison between analytically and numerically determined eigenvalues (columns 2 and 5) for the conditions of Table III, with the latter determined by quartic interpolation. The agreement in Table IV is to within better than 0.1 cm^{-1}. Thus by interpolation the resolution implied by Eq. (12) had been improved by at least a factor of 3.

The numerically determined mode delays $\partial\beta_n'/\partial\omega$, for a 20% variation in ω, are also displayed in Table IV relative to the constant $\Delta n_1^2/n_0c$. The numerical values show an rms deviation of 7.4 psec/km from the correct null value. Numerically and analytically determined values of $\partial\beta_n/\partial\omega$ are displayed in columns 4 and 6, indicating a 7.2-psec/km rms deviation between the two sets of values.

The accuracy of the correlation-function method is clearly better than the field-squared method. Thus the correlation-function method is to be preferred for reasons of both accuracy and simplicity.

Table IV. Comparison of Analytically and Numerically Determined Propagation Constants and Mode Delays[a]

	Numerical			Analytical		
n	β_n' (cm^{-1})	$\frac{\partial\beta_n'}{\partial\omega} - \frac{\Delta n_1^2}{n_0c}$ (psec/km)	$\frac{\partial\beta_n}{\partial\omega} - \frac{\Delta n_1^2}{n_0c}$ (psec/km)	β_n' (cm^{-1})	$\frac{\partial\beta_n}{\partial\omega} - \frac{\Delta n_1^2}{n_0c}$ (psec/km)	
0	1277.24	−3.23	−457.9	1277.24	−454.8	
2	1196.26	11.36	−443.1	1196.29	−454.3	
4	1115.30	−6.95	−456.9	1115.34	−450.0	
6	1034.33	−2.96	−444.8	1034.39	−441.9	
8	953.36	8.97	−421.0	953.44	−430.0	
10	872.40	−7.20	−421.2	872.49	−414.2	
		(rms error, 7.4 psec/km)	(rms error, 7.2 psec/km)			

[a] Numerical values of propagation constants were determined from location of peaks in correlation function, mode delays using Eq. (10).

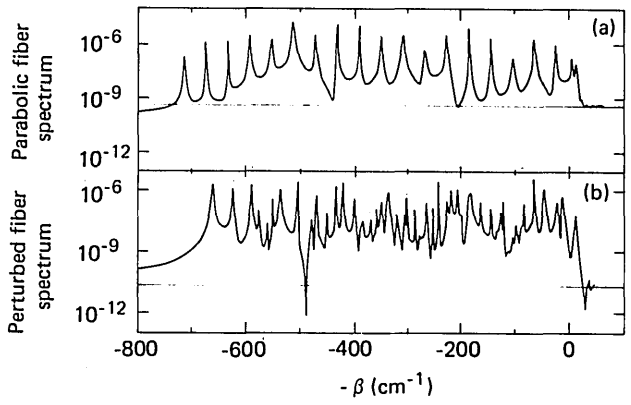

Fig. 3. Field spectrum for transverse position 5 μm from fiber axis. (a) Quadratic variation of index with radius, (b) quadratic variation with radius but with parabolically shaped dip in center. Leaky modes have been suppressed.

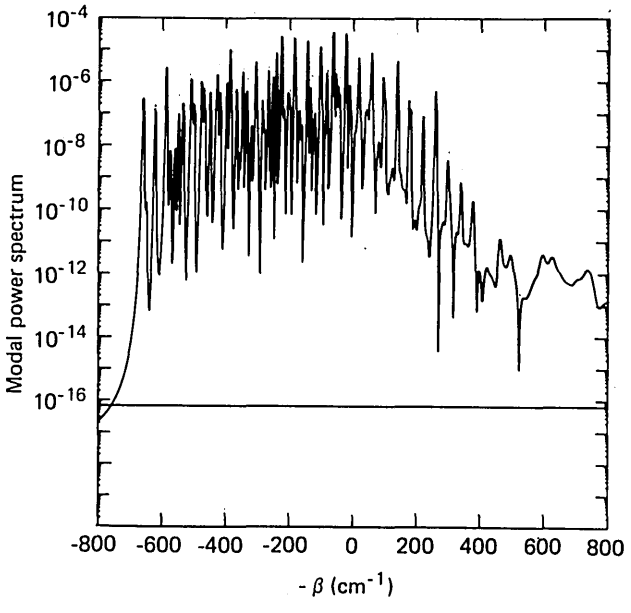

Fig. 4. Fourier transform of complex field-correlation function for fiber with dip, illuminated by beam composed of randomly phased plane waves. Spectrum furnishes both frequencies and amplitudes of modes excited. Leaky modes are also included.

IV. Numerical Illustration

The principles developed in the previous sections have been applied to a fiber with the following refractive index profile:

$$n^2(r) = \begin{cases} n_1^2\left(1 - 2\Delta\left\{\left(\frac{r}{a}\right)^2 - h\left[1 - \left(\frac{r}{R}\right)^2\right]\right\}\right) r \le R \\ n_1^2\left[1 - 2\Delta\left(\frac{r}{a}\right)^2\right] R \le r \le a \\ n_1^2\,(1 - 2\Delta) = n_0^2\, r \ge a \end{cases}, \quad (29)$$

where $\Delta = 0.008$, $h = 0.3$, $R = 6.25$ μm, $a = 31.25$ μm, and $n_0 = 1.5$. The fiber is also assumed to be enclosed in a strongly absorbing jacket[1] at $r = 62$ μm. For the above profile the core index is quadratic in r except for a parabolically shaped dip at the center. A plot of $n(r)$ is shown in Fig. 2. The fiber is assumed to be illuminated with a beam composed of randomly phased plane waves[1] at a wavelength of 1 μm.

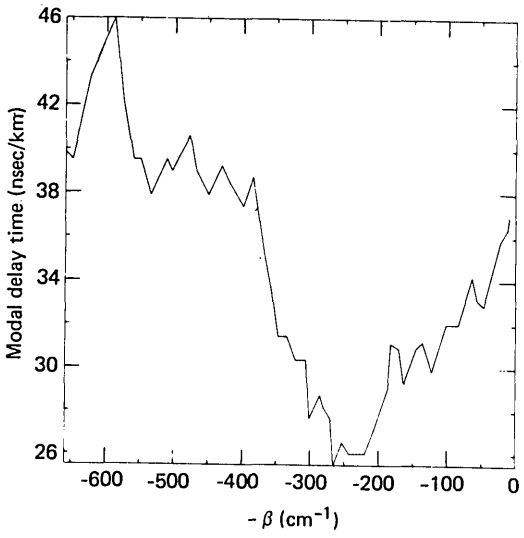

Fig. 5. Mode-group delays for fiber with dip plotted against negative of propagation constant.

The spectrum $|\mathcal{E}'(x,y,\beta)|^2$, corresponding to a propagation distance of 2.5 cm and a transverse position 5 μm from the fiber axis, is shown in Fig. 3(b). Because of the off-axis position all modes are represented. For comparison the spectrum for the same fiber with the central dip eliminated is displayed in Fig. 3(a). For the profile with no dip there are eighteen distinct guided-mode groups, while the less degenerate spectrum for the fiber with the dip shows forty-nine distinct guided-mode groups. Moreover, the dip alters the mode spectrum in a fundamental way that cannot be characterized simply as a perturbation.[22]

The fiber power spectrum $\mathcal{P}_1(\beta)$, calculated from $\langle \mathcal{E}'^*(x,y,0)\mathcal{E}'(x,y,z)\rangle$ with a four-term Blackman-Harris window, is displayed in Fig. 4 for the profile with dip. The heights of the peaks are, of course, proportional to the power excited in the individual modes. Figure 4 also shows the presence of leaky modes, which, however, are disregarded in the computation of dispersion, since previous calculations show that leaky modes can decay in a short distance if a strongly absorbing outer jacket is present.[1] Values of the eigenvalues β'_n were obtained by quartic interpolation from $\mathcal{P}_1(\beta)$, and the derivatives $\partial\beta'_n/\partial\omega$ were determined as $\Delta\beta'_n/\Delta\omega$ from the results of two separate calculations at wavelengths of 1 μm and 0.8 μm, respectively. Equation (10) was then used to compute the modal delays $\partial\beta_n/\partial\omega$, which are shown in Fig. 5 plotted against $-\beta_n$. The modal delays were found to be insensitive

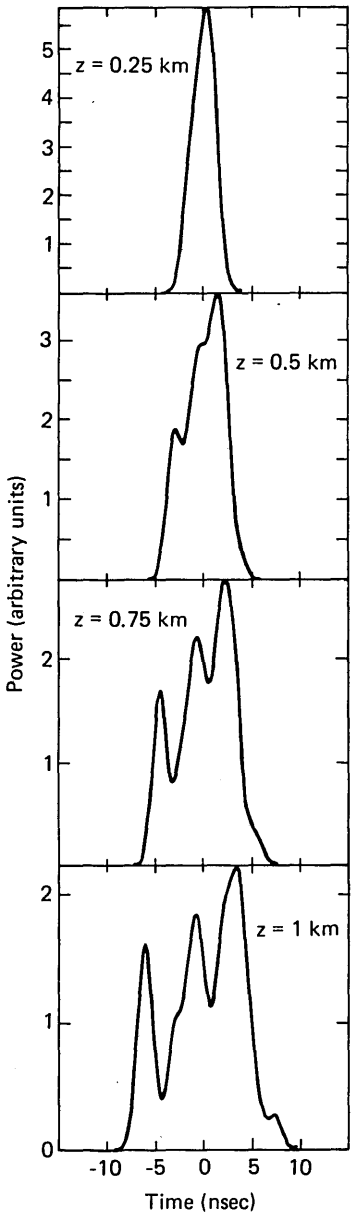

Fig. 6. Effect of dispersion of initially Gaussian pulse with e^{-1} intensity width of 1 nsec.

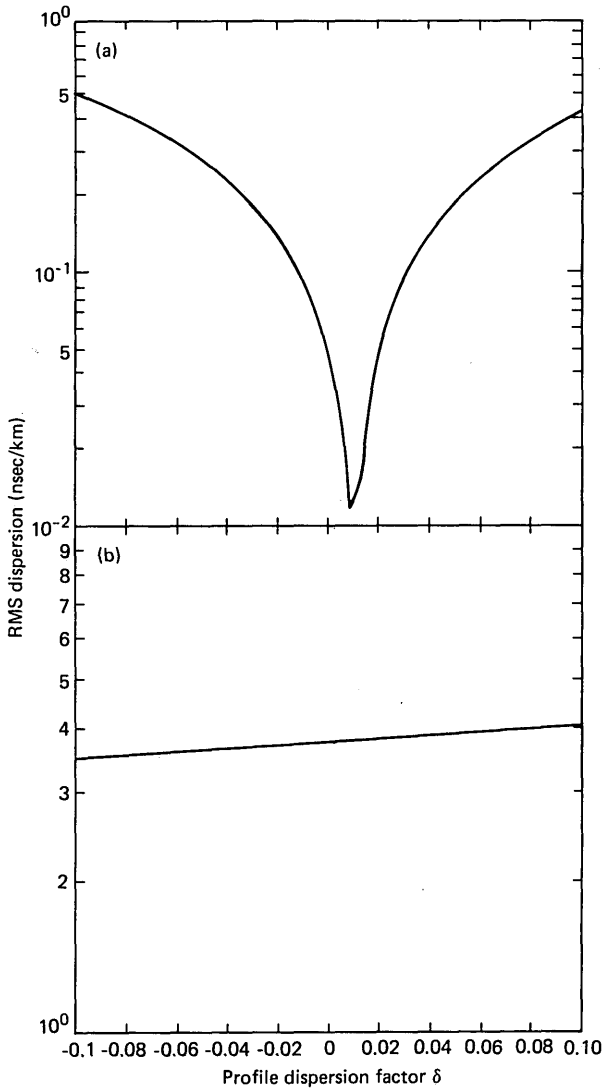

Fig. 7. Plots of rms dispersion against dispersion parameter $\delta = \lambda\partial \ln \Delta/\partial\lambda$.

(a) Quadratic profile,
(b) quadratic profile with dip.

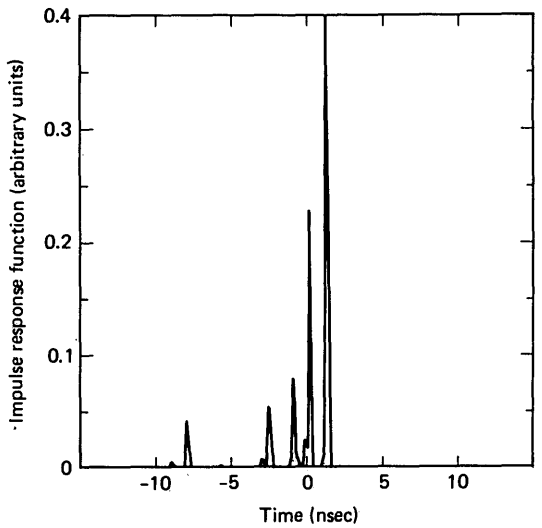

Fig. 8. Impulse-response function at 1 km for fiber with dip assuming illumination with fundamental mode for fiber without dip.

to halving the wavelength interval, to the propagation distance, and to whether the eigenvalues β'_n were determined with or without interpolation. Therefore, the jagged appearance of Fig. 5 can be assumed real and due to the discrete nature of the mode spectrum.

The rms pulse dispersion per unit propagation distance is given by $\sigma = (\langle\tau^2\rangle - \langle\tau\rangle^2)^{1/2}$, where $\langle\tau^m\rangle$ is determined from the relation

$$\langle\tau^m\rangle = \sum_n W_n(v_n)^{-m}, \tag{30}$$

and summation is over strictly guided modes. The dispersion corresponding to Figs. 4 and 5 is $\sigma = 3.67$ nsec/km. The evolution with distance of an initially Guassian-shaped pulse with an initial e^{-1} intensity width of 1 nsec, calculated with the impulse-response function (I.1) and the convolution (I.3), is shown in Fig. 6.

In Fig. 7 the rms dispersion plotted against the profile dispersion parameter[21] $\delta = \lambda\partial \ln \Delta/\partial\lambda$ is shown for (a) the profile without a dip and (b) the profile with dip. It is seen that the profile with dip is far less sensitive to profile dispersion than the profile without dip.

The calculated dispersion corresponding to Figs. 4 and 5 is rather large by experimental standards, but so too is the assumed ratio $R/a \approx 0.2$. However, the modal weights excited by the randomly phased beam also play a role in the large calculated value of dispersion. In order to test the effect of mode excitation on dispersion, the fiber with dip was assumed to be illuminated by a beam having the Gaussian shape

$$\mathcal{E} = \exp[-(x^2 + y^2)/2\sigma_a^2],$$

where σ_a is determined by Eq. (23). This is, of course, a good approximation to the fundamental mode for the fiber without a dip. The impulse-response function at 1 km for the fiber with dip corresponding to this illumination is shown in Fig. 8, where it is evident that relatively few modes are excited. The most prominent peak in Fig. 8 corresponds to the fundamental mode. The peaks have been arbitrarily given a Gaussian shape with a $1/e$ width of 100 psec. The rms dispersion for this impulse response function is 2.24 nsec/km. However, this number is rather deceiving, since an important contribution to σ comes from the group of trailing modes containing little energy. If, for example, only the first four mode groups which contain 87% of the pulse power are considered, the dispersion reduces to 0.732 nsec/km.

The intensity as a function of radius at $z = 2.45$ cm resulting from the Gaussian beam illumination is shown in Fig. 9. This should be compared with Fig. 10, which shows the intensity distribution of the fundamental mode for the profile with dip, determined from a solution of Eq. (5) with iz substituted for z. Replacement of z by iz causes the normal mode solutions [Eq. (7)] to grow exponentially. The largest β'_n value corresponds to the fundamental mode. Consequently that mode will prevail over the others after a sufficiently large propagation distance. In the present case that distance is of the order of 2 cm.

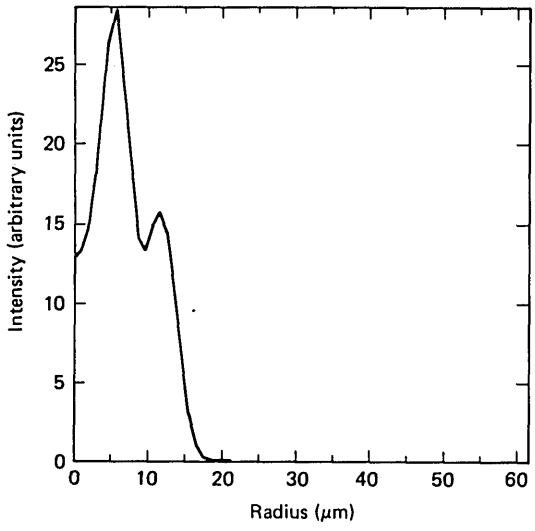

Fig. 9. Intensity distribution at $z = 2.45$ cm; same conditions as in Fig. 8.

V. Conclusions

It has been previously shown that a propagating-beam solution of a scalar wave equation based on a discrete Fourier representation provides an accurate discription of the spatial and angular properties of the electric field in an optical waveguide.

In this paper we have shown how the same computation can also furnish accurate and detailed information on both the axial or mode spectrum and the relative power excited in various modes under general launch conditions. This information can be used to compute the impulse response and the pulse dispersion for a fiber of general refractive index profile. The latter computations, however, require a minimum of two propagation calculations, since group delays must be computed by a numerical evaluation of the derivatives of mode eigenvalues with respect to frequency.

Naturally the accuracy with which mode propagation constants and weights can be computed increases with the propagation distance encompassed in a given calculation. However, we have determined that with the help of digital signal-processing techniques, accurate information can be gained from propagation distances of the order of centimeters.

The propagating-beam method thus provides an accurate and unified description of most phenomena of current interest associated with optical waveguides.

This work was performed under the auspices of the U.S. Department of Energy by the Lawrence Livermore Laboratory under contract W-7405-ENG-48.

Appendix: Treatment of Profile Dispersion

If we make use of Eq. (16) and keep only terms to first order in Δ, we can write the parabolic equation (5) as

$$2ik\frac{\partial\mathcal{E}'}{\partial z} = \nabla_1^2\mathcal{E}' + 2\Delta n_1^2\left(\frac{\omega}{c}\right)^2\left[1 - f\left(\frac{r}{a}\right)\right]\mathcal{E}'. \tag{A1}$$

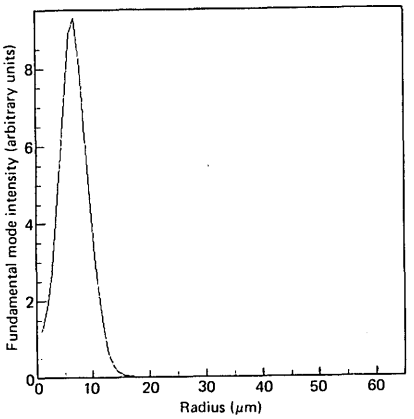

Fig. 10. Intensity distribution of fundamental mode for propagation in fiber with dip obtained by solving Eq. (5) with z replaced by iz.

Substitution of $\mathcal{E}' = u_n'(\mathbf{x})\exp(-i\beta_n' z)$ into Eq. (A1) gives

$$2\beta_n' k u_n' = \nabla_t^2 u_n' + 2\Delta n_1^2 \left(\frac{\omega}{c}\right)^2 \left[1 - f\left(\frac{r}{a}\right)\right] u_n'. \tag{A2}$$

It will be assumed that $f(r/a)$ is independent of ω but that the material parameters n_0, n_1, and Δ can vary with ω.

From first-order perturbation theory,[23] one has

$$\frac{\partial}{\partial\omega}\left(\beta_n' n_0 \frac{\omega}{c}\right) = \frac{\partial}{\partial\omega}\left[\Delta n_1^2 \left(\frac{\omega}{c}\right)^2\right] \left\langle n \left| 1 - f\left(\frac{r}{a}\right) \right| n \right\rangle, \tag{A3}$$

where

$$\left\langle n \left| 1 - f\left(\frac{r}{a}\right) \right| n \right\rangle = \iint u_n'^2(\mathbf{x}) \left[1 - f\left(\frac{r}{a}\right)\right] dx dy. \tag{A4}$$

Let us call $\beta_n'^0$ the eigenvalue of Eq. (A2) for no variation of the material parameters with ω. In that case Eq. (A3) becomes

$$n_0\left(\frac{\beta_n'^0}{c} + \frac{\omega}{c}\frac{\partial\beta_n'^0}{\partial\omega}\right) = \Delta n_1^2 \frac{2\omega}{c^2} \left\langle n \left| 1 - f\left(\frac{r}{a}\right) \right| n \right\rangle. \tag{A5}$$

Equation (A5) can be used to eliminate the matrix element, $\langle n|1 - f(r/a)|n\rangle$, from Eq. (A3). When this is done, Eq. (A3) becomes

$$\frac{\partial\beta_n'}{\partial\omega} = \frac{\partial\beta_n'^0}{\partial\omega}\left[1 + \frac{\omega}{2}\frac{\partial \ln(\Delta n_1^2)}{\partial\omega}\right] + \beta^0\left[\frac{1}{2}\frac{\partial \ln(\Delta n_1^2)}{\partial\omega} - \frac{\partial \ln n_0}{\partial\omega}\right]. \tag{A6}$$

Equation (A6) can also be expressed in terms of derivatives with respect to wavelength as

$$\frac{\partial\beta_n'}{\partial\omega} = \frac{\partial\beta_n'^0}{\partial\omega}\left(1 - \lambda\frac{\partial \ln n_1}{\partial\lambda} - \frac{1}{2}\lambda\frac{\partial \ln\Delta}{\partial\lambda}\right) + \frac{\beta_n'^0}{\omega}\left(\frac{1}{2} + \frac{\Delta}{1-\Delta}\lambda\frac{\partial \ln\Delta}{\partial\lambda}\right). \tag{A7}$$

References

1. M. D. Feit and J. A. Fleck, Jr., Appl. Opt. **17,** 3990 (1978).
2. R. Olshansky and D. B. Keck, Appl. Opt. **15,** 483 (1976).
3. D. Gloge and E. A. J. Marcatili, Bell Syst. Tech. J. **52,** 1563 (1973).
4. J. J. Ramskov Hansen and E. Nicolaisen, Appl. Opt. **17,** 2831 (1978).
5. J. J. Ramskov Hansen, Opt. Quantum Electron. **10,** 521 (1978).
6. R. Olshansky, Appl. Opt. **15,** 782 (1976).
7. S. Choudhary and L. B. Felsen, J. Opt. Soc. Am. **67,** 1192 (1977).
8. J. A. Arnaud and W. Mammel, Electron. Lett. **12,** 6 (1976).
9. J. G. Dil and H. Blok, Opto-electronics **5,** 415 (1973).
10. A. G. Gronthoud and H. Blok, Opt. Quantum Electron. **10,** 95 (1978).
11. T. Tanaka and Y. Suematsu, Trans. IECE Jpn. **E59,** 11 (1976).
12. D. Gloge, Bell Syst. Tech. J. **51,** 1765 (1972).
13. See also discussion by J. Arnaud, Electron. Lett. **14,** 663 (1978).
14. For a thorough discussion of the use of windows in numerical Fourier analysis, see F. J. Harris, Proc. IEEE **66,** 51 (1978).
15. George N. Kamm, J. Appl. Phys. **49,** 5951 (1978).
16. D. Marcuse, *Light Transmission Optics* (Van Nostrand-Reinhold, New York, 1972).
17. The truncation of the square-law refractive index profile may perturb the eigenvalue near cutoff. However, this effect cannot be detected within the resolution of these calculations.
18. D. Gloge, I. P. Kaminow, and H. M. Presby, Electron. Lett. **11,** 471 (1972).
19. The Hanning truncation function is $(\frac{1}{2} - \frac{1}{2}\cos 2\pi z/Z)$, where Z represents the length of the window.
20. The four-term Blackman-Harris window can be represented as $(0.35875 - 0.48829\cos 2\pi z/Z + 0.14128\cos 4\pi z/Z - 0.01168\cos 6\pi z/Z)$.
21. Slightly different profile dispersion parameters have been defined by other workers; see, for example, Refs. 2 and 18.
22. A correct application of first-order perturbation theory will give a splitting of the degenerate levels in the mode spectrum in addition to level shifts. This correct procedure, which requires picking a linear combination of degenerate mode eigenfunctions as the unperturbed functions through the diagonalization of a matrix, has unfortunately not been followed in most of the applications of perturbation theory to graded-index fibers. The point in the present example is that the perturbation clearly gives large level shifts in addition to level splitting. For a discussion of perturbation theory involving degenerate states, see, for example, P. M. Morse and H. Feshbach, *Methods of Theoretical Physics* (McGraw-Hill, New York, 1953), p. 1673.
23. For a more complete discussion of the underlying principle, see J. Arnaud, *Beam and Fiber Optics* (Academic, New York, 1976), pp. 216–218.